Reprinted from *J. Mol. Biol.* (1977) **114**, 491–506

Packing of Ribosomes in Crystals from the Lizard *Lacerta sicula*

P. N. T. Unwin and C. Taddei

J. Mol. Biol. (1977) **114**, 491–506

Packing of Ribosomes in Crystals from the Lizard *Lacerta sicula*

P. N. T. Unwin

Medical Research Council Laboratory of Molecular Biology
Hills Road, Cambridge, CB2 2QH, England

and

C. Taddei

Institute of Histology and Embryology
Electron Microscopy Centre
University of Naples, 80134 Naples, Italy

(Received 3 March 1977)

The packing of ribosomes in the large crystalline sheets found in the lizard *Lacerta sicula* has been investigated by electron microscopy. The ribosomes in each of the two layers composing a sheet are organised as tetramers on a *P*4 space group lattice. The two layers face in opposite directions and tend to be related to one another crystallographically, generating a family of *P*422 crystals of different unit cell dimensions. The projected structure of one layer was determined from negatively stained, isolated sheets by separating the contributions from each layer in Fourier transforms computed from electron micrographs. Comparison of the projection map with other, low resolution, analyses of images of isolated eukaryotic ribosomes indicates that the large subunit–small subunit axis lies approximately parallel to the plane of the sheet.

1. Introduction

Large crystalline sheets of ribosomes are formed in the follicle cells and in the oocytes of the lizard *Lacerta sicula* during the winter hibernation period (Taddei, 1972) or in the summer months after cold treatment (Taddei *et al.*, 1973). The sheets tend to aggregate, partially oriented, into clumps or "ribosomal bodies", attaining diameters of up to about 15 μm after a prolonged spell at low temperature. Structurally, these sheets appear to be similar to those found in chick embryos subjected to hypothermia (Byers, 1967) or in dying chick nerve cells (O'Connor & Wyttenbach, 1974), and both in the lizard (Taddei *et al.*, 1973) and the chicken (Morimoto *et al.*, 1972*b*) they constitute a large pool of ribosomes which are not engaged in protein synthesis. The lizard sheets differ, however, in that they are always associated with membranes (cisternae) and only occur extensively as double layers (Fig. 1). Chick embryo sheets are not associated directly with membranes and occur both as single layers and as multi-layer stacks. In either animal, the ribosomes of any one layer are organised as tetramers on a *P*4 space group lattice.

It is shown here that the two layers of ribosomes comprising a sheet, in the lizard, tend to be related to each other in a number of specific ways. They generate a family of crystals having the same space group symmetry, *P*422, but having different unit

cell dimensions. That crystal having the smallest unit cell dimension corresponds to the crystal in chick embryos described by Byers (1967), but it is possible that the range of crystals which we have found in the lizard is a ubiquitous feature of all ribosome crystals of this type.

Although superposition of the two layers in isolated sheets gives rise to complex moiré effects, the contributions from each layer can easily be separated by Fourier analysis. We are thus able to determine the projected density distribution of the ribosomes composing one layer.

2. Methods

(a) *Isolation procedure*

All isolation steps were carried out in a cold room at ~4°C, using summer or autumn female lizards which had been kept at this temperature for at least a fortnight. Each lizard contained 5 to 15 previtellogenic oocytes of about 1 mm diameter.

The cytoplasms from about 10 of these oocytes were carefully opened out, with the aid of a dissecting microscope, into small drops (~5 μl) of a medium consisting of 100 mM-KCl, 5 mM-$MgCl_2$, 5 mM-triethanolamine·HCl, 0·25 M-sucrose (pH 7·6). The drops were collected together in a small tube, stirred vigorously, and centrifuged at 300 *g* for 10 min, producing a small pellet consisting mainly of large ribosomal bodies. After resuspending this pellet in about 50 μl of the same medium, the sheets were released by adding 10 μl of 1% (v/v) Triton X100 (Koch-Light Ltd., Bucks, England) in this medium and then shaking. The concentrated suspension of isolated sheets was then diluted into ~1 ml of a medium consisting of 100 mM-KCl, 10 mM-$MgCl_2$, 5 mM-triethanolamine·HCl, 1% (v/v) glutaraldehyde (pH 7·6), containing a small number of Biobeads SM-1 (Bio-Rad Laboratories, Richmond, California) to absorb the excess Triton (Holloway, 1973). The diluted suspension was allowed to stand for at least 3 or 4 h before applying to microscope grids.

(b) *Electron microscopy and image processing*

Support films for the isolated sheets were prepared by floating carbon off mica onto 600-mesh copper grids (Polaron Equipment Ltd, Watford, England). Only freshly prepared films were used. The suspension of sheets was applied to the mica side of the support films by first putting small quantities into PTFE cups, placing a grid on top of each cup, then inverting the whole assemblies to allow the sheets to settle out over a period of several hours. Uranyl acetate (2%, w/v) containing a small amount of cytochrome *c* (about 2 mg/ml) was used as the negative stain.

The sheets were examined at 11,000× in a Philips EM301 electron microscope operating at 100 kV, and having an objective aperture of semi-angle 5×10^{-3} radians. Care was taken to minimise radiation damage, although the appearance of the sheets was not significantly changed by the irradiation. Images were recorded sufficiently close to focus (within about 5 μm) that the major contribution to the low resolution detail (spacings greater than 90 Å) was from amplitude contrast, and the contrast transfer function was fairly uniform over the range of object spacings of interest (Erickson & Klug, 1971).

Micrographs were selected and analysed qualitatively by optical diffraction. More quantitative analysis was carried out by densitometering them at 30-μm intervals (30 μm spot size) with a modified Nikon comparator (Arndt *et al.*, 1969) and computing Fourier transforms of these optical density arrays. The Fourier transform program, which was written by Dr L. Amos, is similar to that described by DeRosier & Moore (1970), but designed to operate on a 512×512 array size. The measurements were taken over an area of only half to three-quarters of this size and a "floating" procedure (DeRosier & Moore, 1970) was applied before doing the Fourier transformation.

Comparison of the fall-off in computed diffraction intensities with the fall-off of intensities found in X-ray patterns from pellets of ribosomal bodies (Unwin, unpublished results) indicated that a substantial degree of *short range* disorder was present in the negatively stained isolated sheets. To compensate for this, a "temperature factor" correction was applied in the Fourier synthesis which had the effect of emphasising the

higher spacings in the object to a similar degree as is normally achieved in higher resolution images of negatively stained objects at moderate levels of defocus (Erickson & Klug, 1971).

3. Results

(a) *Ribosomal bodies*

Thin sections through ribosomal bodies have been described in an earlier publication (Taddei, 1972), but it is useful to summarise here these observations and enlarge on certain aspects.

A cross-sectioned view of a ribosomal body (Fig. 1(a)) shows numerous double layer sheets of ribosomes, bordered on either side by a membrane and lying in close proximity to one another in nearly parallel orientation. The ribosomes within the sheets superimpose in this view to form dotted, broken or continuous lines of higher than average density. The appearance of these lines varies according to the orientation of the layers with respect to the section and section thickness (see Byers, 1967). Often a region of dense "matrix" material (also found in the chick embryo crystals) can be clearly distinguished between the double layers composing a sheet (M in Fig. 1(a), and see Taddei & Filosa, 1976). The separation of the double layers is somewhat variable, but it is not clear whether this is due mainly to differences in the amount of matrix material between them, to differences in bonding relationships, or to fixation artefacts.

An oblique view of a ribosomal body, in which the thin section is cut roughly parallel to the sheets, shows a series of bands of tetramers arranged in the $P4$ configuration, and alternating in hand as one crosses the field (Fig. 1(b)). The repeating unit consists of a membrane, a sheet made up from two bands of tetramers in the $P4$ configuration, each of opposite hand, and one further membrane. The change in handedness of the two layers within a sheet suggests that the ribosomes in each layer are packed in an identical manner but face in opposite directions, i.e. that they present the same surface to the membranes against which they are juxtaposed. Whether the first layer of a sheet appears as right or left-handed as one traverses the field in a given direction therefore depends on how the sheets are inclined with respect to the section. If they are inclined one way, the first layer will be that with the juxtaposed membrane beneath it; if they are inclined the other way, the first layer will be that with the juxtaposed membrane above it.

The nature of the inclination of the sheets with respect to an oblique section can easily be determined by tilting the section through a series of small angles and observing whether they become foreshortened or expanded in the direction perpendicular to the tilt axis. We have established from such an experiment that the right-handed layer is the one having the juxtaposed membrane beneath it. Going towards the right in Figure 1(b), the first layers of all the sheets are seen to be right-handed; these sheets are therefore all inclined downwards in this direction, as if the section were cut along the line drawn in Figure 1(a) and were looked at from above.

At first sight it may seem that the majority of the double layers comprising the sheets are randomly oriented with respect to one another. However, closer inspection of oblique views indicates that this is not so. We find that the two layers of a sheet tend to be rotated with respect to one another through certain specific angles. The angles, and the centres of rotation, are such that a lattice can be drawn between them on to which certain tetramers in both layers fit exactly. Black squares have

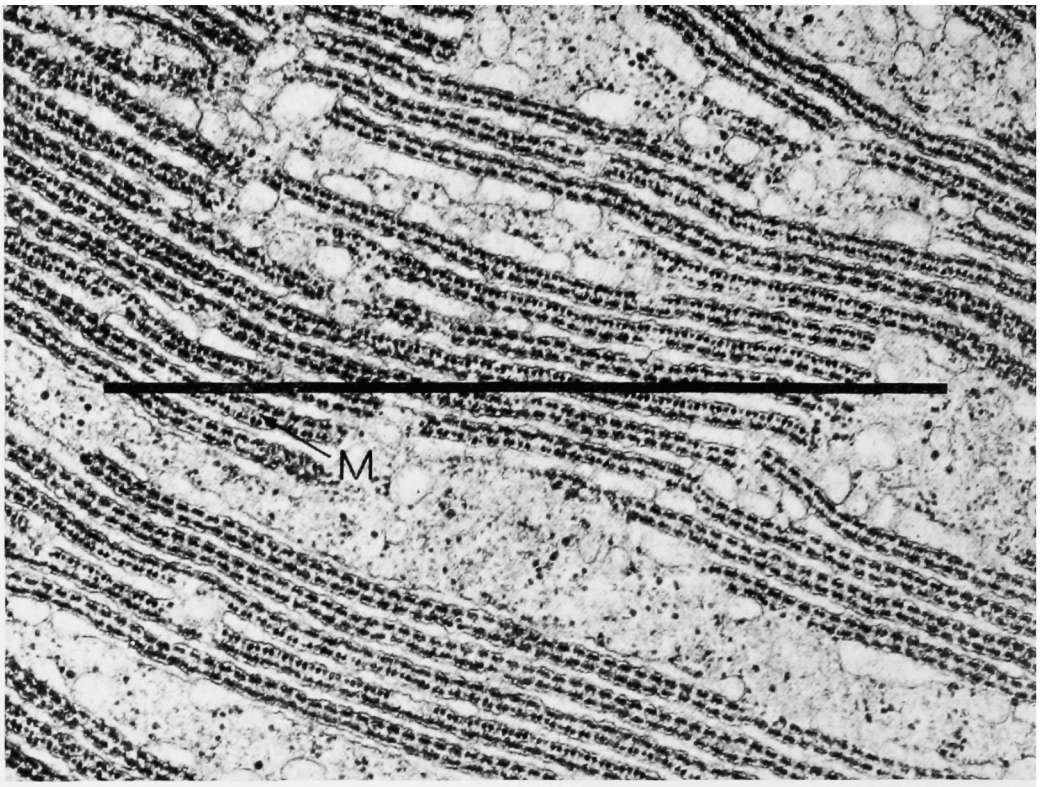

(a)

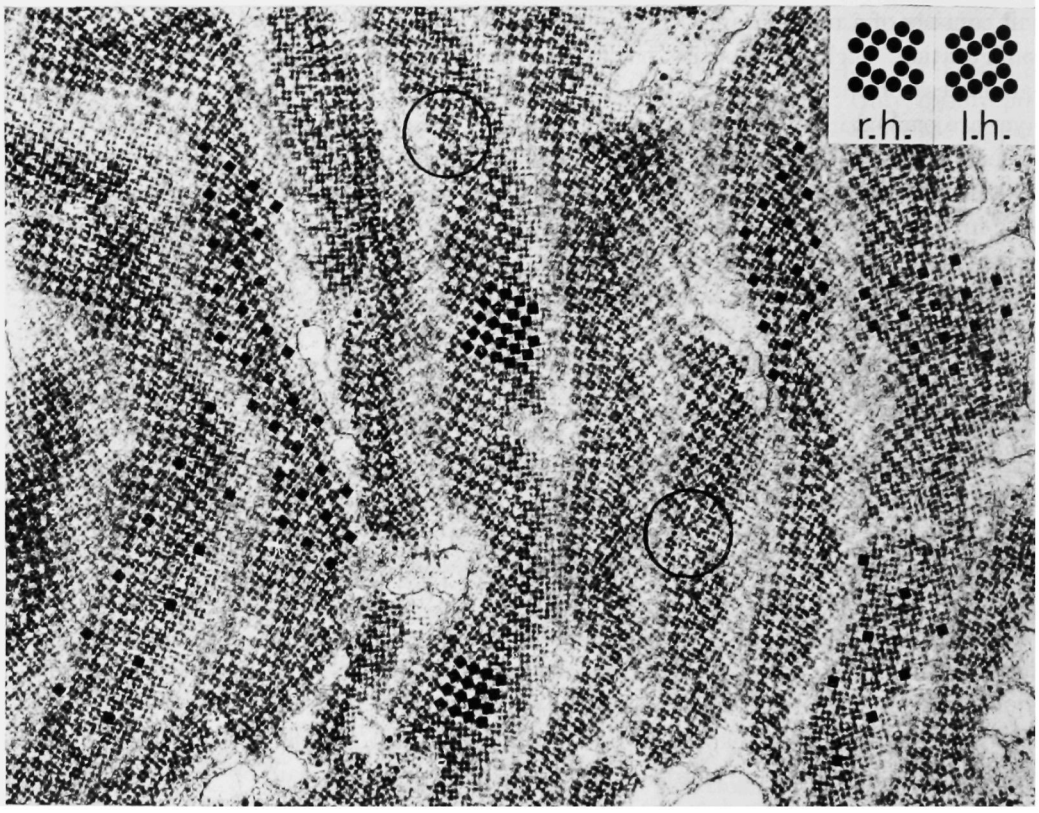

(b)

been drawn over tetramers in Figure 1(b) to identify some of the lattices; all such lattices are based on a square network and all have a unit cell size which is equal to or greater than that of one layer.

These lattices which are shared by both layers are analogous to the "coincidence lattices" which are used to relate adjacent metallic crystals to one another in field-ion micrographs (Brandon *et al.*, 1964). There are families of such lattices which have been characterised by the density of coincident sites and the most densely packed planes involved. The lattices we observe are most simply classified in terms of a parameter, Σ, denoting the number of tetramers in either layer per coincidence lattice point (or per coincidence lattice unit cell), and the sense of rotation involved (see below). Figure 1(b) thus gives examples of the Σ_1, Σ_5, Σ_{13} and Σ_{17}-type of lattice.

According to the description given so far, all sheets are composed of two oppositely facing layers of ribosomes, and the ribosomes in each layer are packed in an identical way on a $P4$ lattice. A consequence of this description is that the individual layers, in all those sheets where coincidence lattices can be drawn, are related by two unique 2-fold axes, intersecting at the coincident sites. Each such sheet must therefore represent a true crystal belonging to the space group $P422$. These crystals have a unit cell dimension, in the plane of the sheet, which is $\sqrt{\Sigma}$ times the unit cell dimension of one layer. The accuracy of this description is confirmed by analysis of isolated sheets (see below).

(b) *Isolated sheets*

Sheets isolated according to the procedure given in Methods tend to vary considerably in size and organisation. Those obtained from cooled summer lizards are generally smaller and tend to be polycrystalline in character.

An example of such a sheet, negatively stained, is given in Figure 2. The two layers comprising this sheet are superposed in a variety of ways, giving a variety of rather complex looking patterns. The unit cell dimensions of most of these are consistent with the Σ_1, Σ_5 and Σ_{13} types of coincidence lattice, but there is also an example of a region having a much larger unit cell size (lower right of Fig. 2). Such examples are comparatively rare; the largest unit cell size commonly found is that corresponding to the Σ_{29}-type of lattice.

It is also evident from Figure 2 that the orientation of the lattice of one crystal tends to be simply related to that of its neighbour. The actual relationships involved suggest that the changes in orientation as one crosses the boundary zone are associated with one layer rather than with both. Optical diffraction patterns from isolated polycrystalline sheets and observations of oblique sections (see Fig. 1(b)) confirm this interpretation.

FIG. 1. Thin sections through ribosomal bodies in whole oocytes, prepared as described by Taddei (1972). (a) Cross-sectional view in which the section is cut perpendicular to the sheets of ribosomes. It shows each sheet to be constructed from 2 layers, the outer surfaces of which are lined by membranes. Dense matrix material between the layers is particularly obvious at M. (b) Oblique view in which the section is cut roughly parallel to the sheets, as along the line indicated in (a). The thickness of a sheet is greater than that of the section. The ribosomes in each sheet appear as 2 bands of tetramers arranged on a $P4$ space group lattice and having first a right, then a left-handed configuration (see inset). In several sheets squares have been drawn over certain tetramers to identify lattices which relate the 2 layers to one another (see text). In the 2 regions encircled the orientation of one, but not the other, layer of a sheet changes. This feature and others referred to in the text are best studied by viewing the page at a glancing angle to the eye and lining up along the rows of ribosomes. Magnification of the Figure = 35,000×.

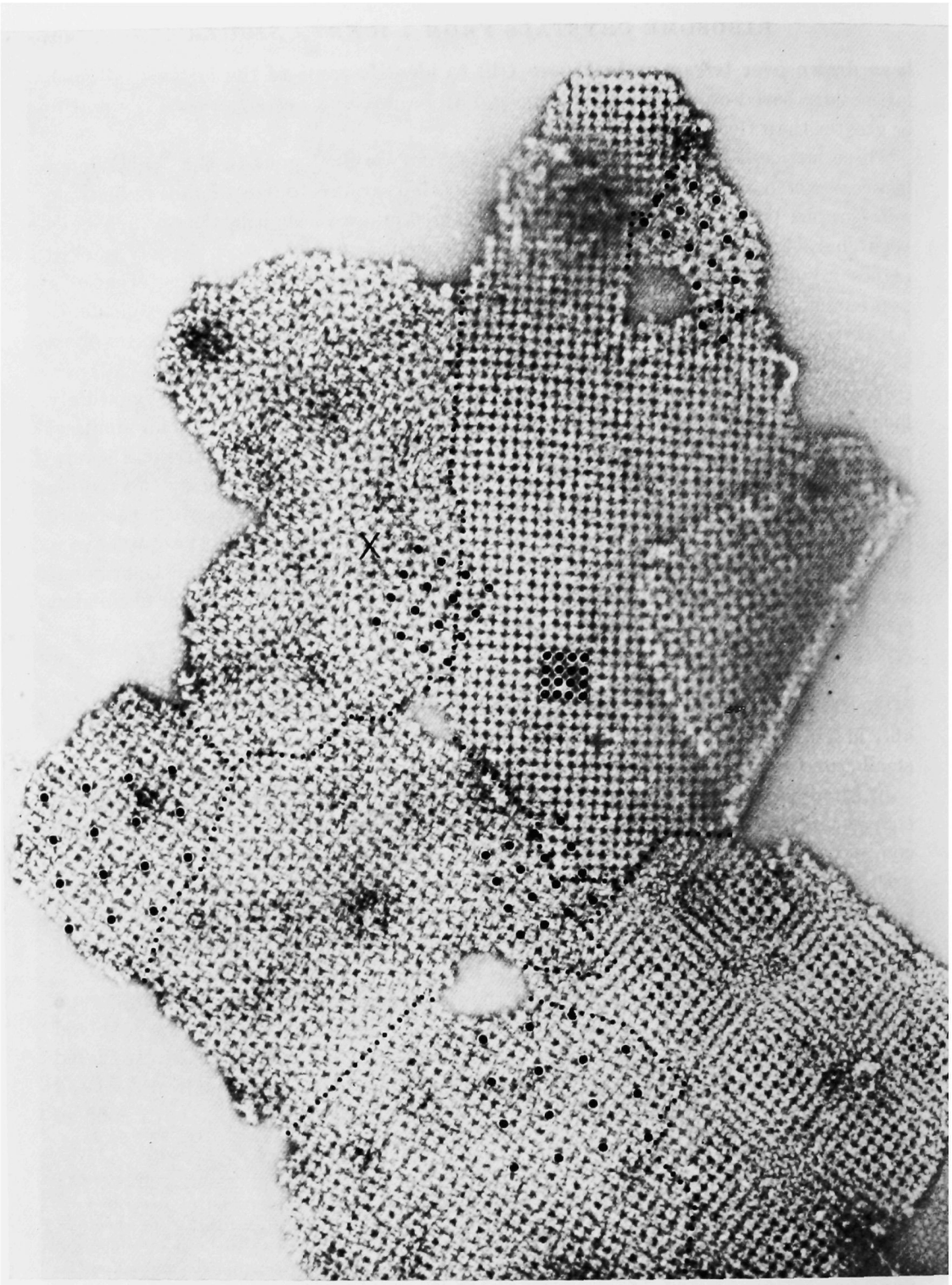

FIG. 2. Isolated sheet of ribosomes from a cooled summer lizard negatively stained with uranyl acetate. In each of the several crystalline patches from which it is built up, the 2 layers give rise to a complex superposition pattern. Dotted lines have been drawn to show the boundaries between the patches, and arrays of dots have been drawn to show that similar lattices can be placed over the patches as in Fig. 1(b). In some regions, such as that marked X, the 2 layers tend to be shifted with respect to each other by small amounts from their positions as expected from cross-sectional views (see text). Magnification = 35,000×.

(c) *Three-dimensional packing arrangements*

A gallery of the most frequently encountered crystals is presented in Figure 3, with the number of tetramers per coincident site, Σ, increasing as one goes down the page. The examples show the two types of crystal it is possible to produce with a given value of Σ by changing the sense of the rotation between the layers.

Table 1 lists all the crystals able to be generated up to a value of Σ equal to 29,

TABLE 1

List of P422 ribosome crystals found in Lacerta sicula

No. of tetramers/ coincident site (Σ)	Unit cell dimension (Å)	Least angle of rotation†	Coincident reciprocal lattice points‡
1	595§	0°	1,0; 0,1; 1,1
5a	1330	+36·9°	2,1; −1,2; 1,3
5b		−36·9°	1,2; −2,1; −1,3
13a	2145	+22·6°	3,2; −2,3; 1,5
13b		−22·6°	2,3; −3,2; −1,5
17a	2453	+28·1°	1,4; −4,1; −3,5
17b		−28·1	4,1; −1,4; 3,5
25a	2975	+16·3°	4,3; −3,4; 1,7
25b		−16·3°	3,4; −4,3; −1,7
29a	3204	+43·6°	2,5; −5,2; −3,7
29b		−43·6°	5,2; −2,5; 3,7

† Positive is clockwise rotation of left-handed configuration over right.

‡ These lie on a square lattice; given are the co-ordinates of the 1,0, 0,1 and 1,1 points of this lattice in terms of the co-ordinates h,k for one layer.

§ Figures based on X-ray measurements (Unwin, unpublished work).

and several of the parameters which are relevant to each. Simple three-tone representations of these crystals were constructed on the basis of the parameters given in this Table and some are shown in Figure 4. Despite the fact that the representations only give a very crude approximation to a projection of the negative stain distribution, close inspection reveals that there is a good correspondence between them and the electron micrographs in Figure 3. Clearly, these micrographs of the isolated sheets are in accord with the classification given in Table 1, and with the thin section results.

No quantitative assessment of the relative abundance of these various types of crystal has been attempted. However it is undoubtedly the smaller unit cell, Σ_1, Σ_{5a}, Σ_{5b}, lattices which are the most common; there is also a preponderance of coincidence lattices where the ribosomes of the superposing tetramers lie directly on top of, rather than between, each other.

Unfortunately not all the isolated sheets we have observed can be categorised as above. Apart from those sheets, already mentioned, having an exceptionally large value for Σ, there are others which form patterns with the expected unit cell

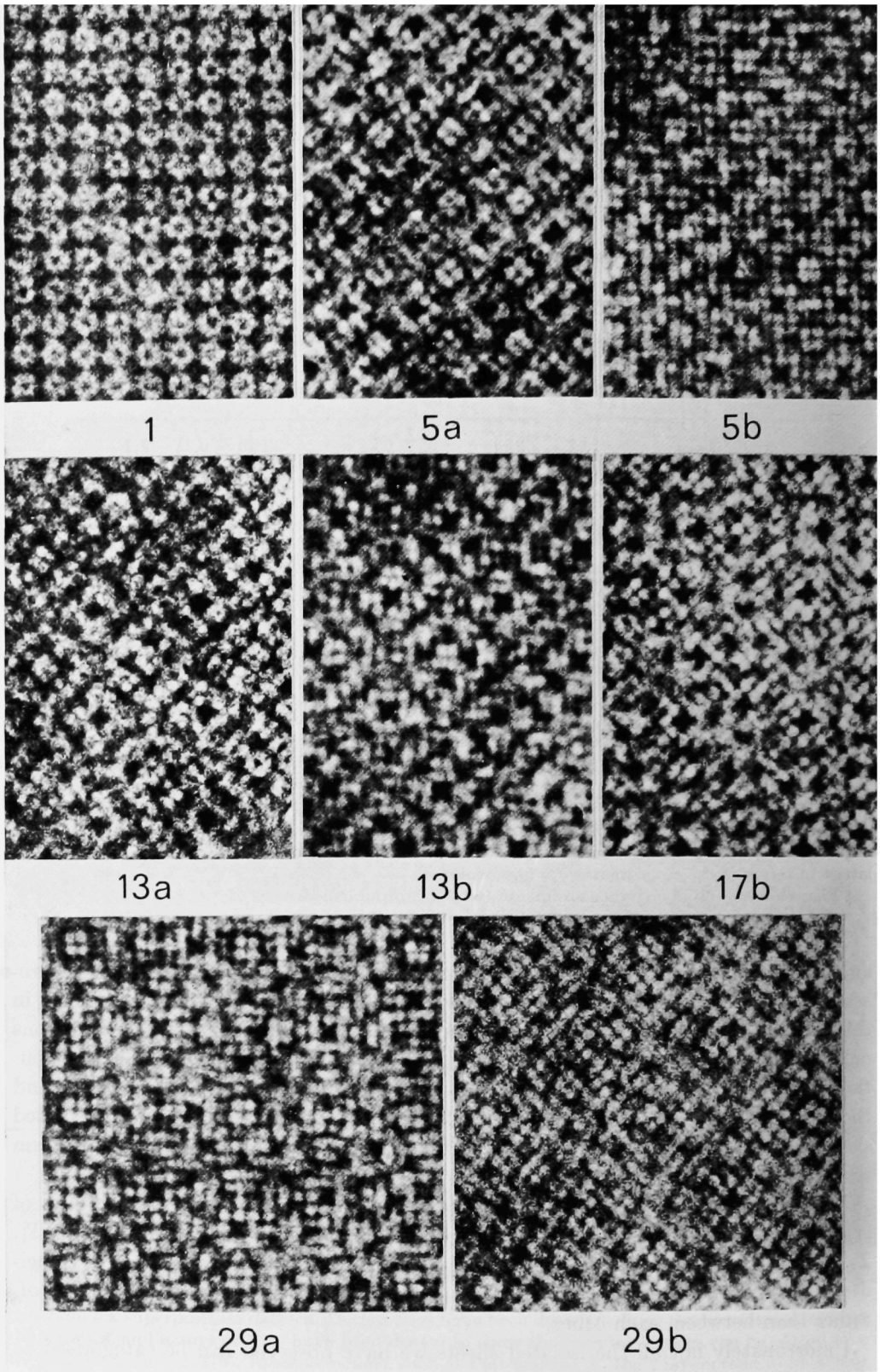

FIG. 3. Some of the most common $P422$ crystals found in the isolated sheets. The plane group symmetry in this projection is p4mm. The patterns formed by these crystals, and their unit cell size, vary according to the relative orientations of the 2 layers (see Table 1 and text). Magnification $= 80{,}000\times$.

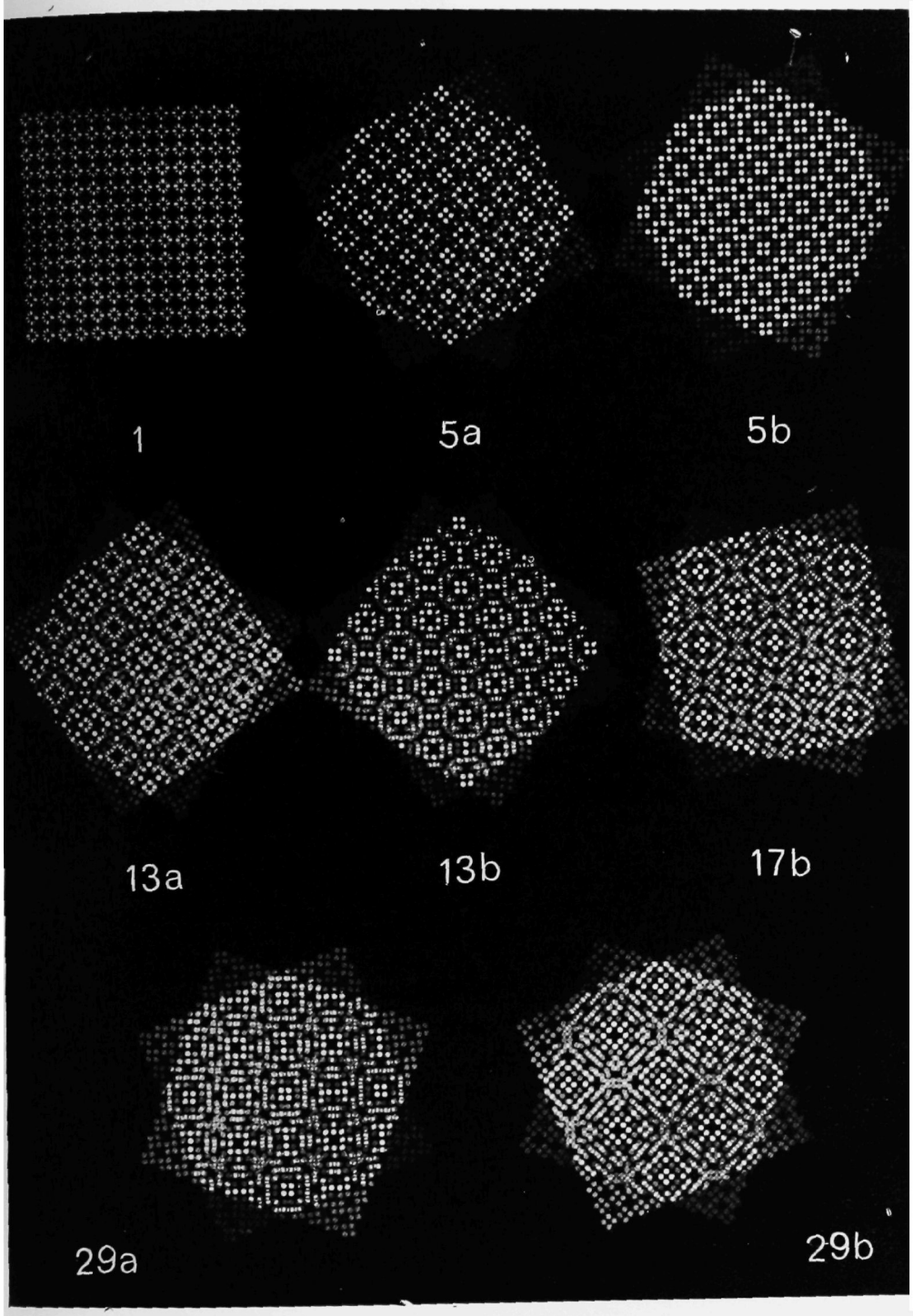

FIG. 4. Simulated images made by rotating 2 patterns, each representing the arrangement of ribosomes in one layer, by the amounts specified in Table 1. The centre of rotation is an intra-tetramer 4-fold axis. These crude representations may be compared with the micrographs in Fig. 3, which are oriented in the same way and are at about twice the magnification.

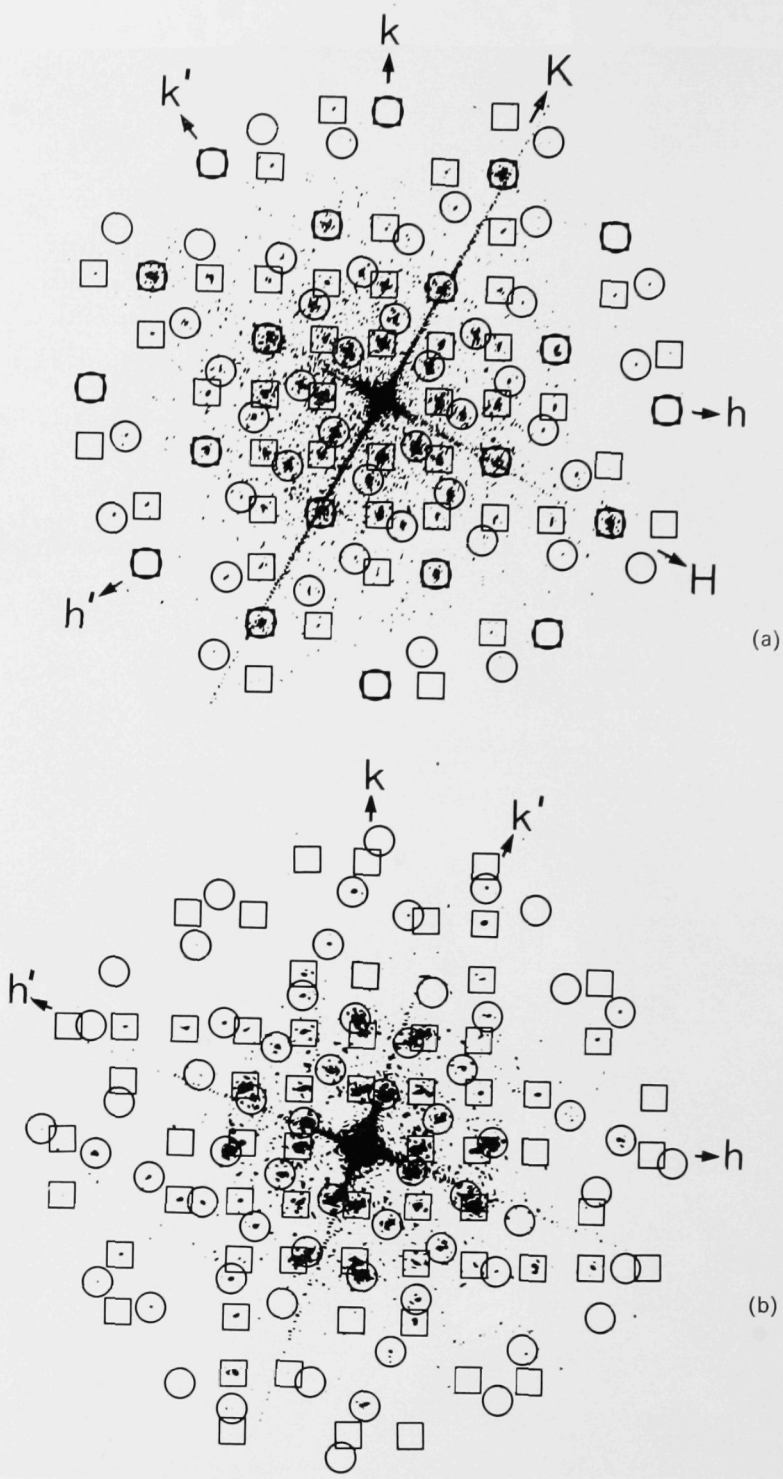

FIG. 5. Optical diffraction patterns from isolated sheets. The rotations of the layers are as for the (a) Σ_{5b}, (b) Σ_{13a}, (c) Σ_{5a}, (d) Σ_{29a} lattices, described in Table 1. Each pattern can be indexed either as if it were from a (2 layer) single crystal, H, K in (a), or as if it were from a pair of (1 layer) crystals: h,k; h′k′. (H and K are along the 2-fold axes).

The spots encircled in (a) and (b) (squares for lattice h,k and circles for lattice h′,k′) refer to

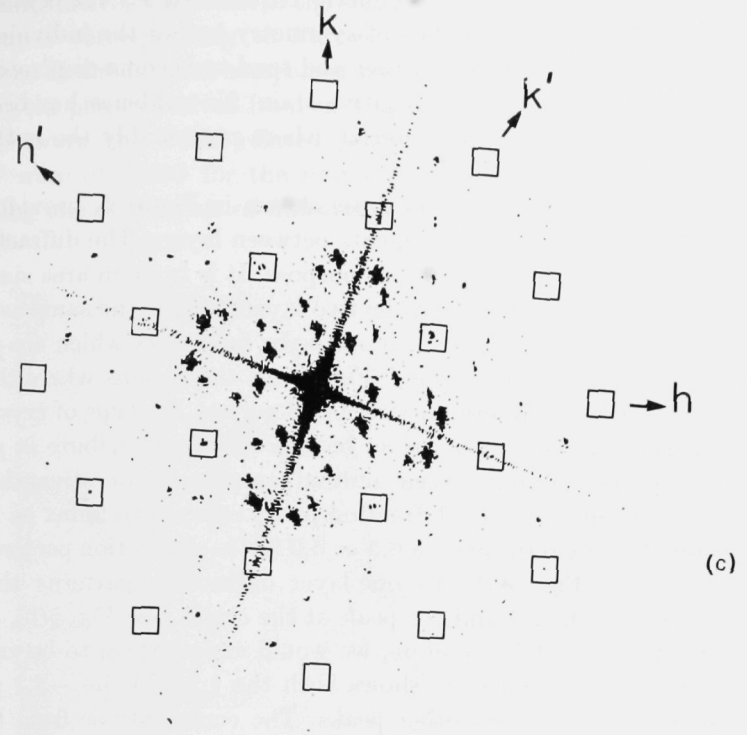

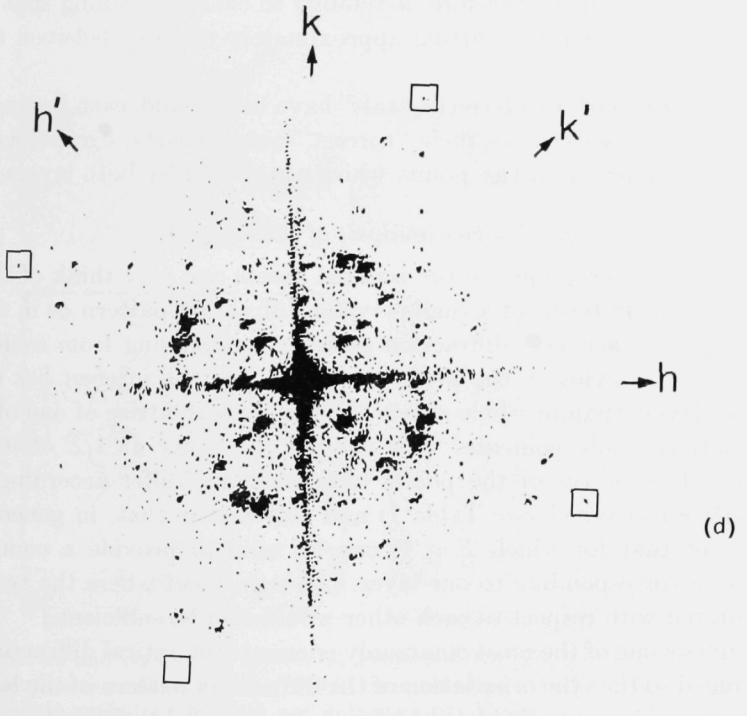

all the peaks able to be measured in the computer analysis (see text). The points at which the one-layer patterns overlap are obvious in (a) (circles over squares), but not in (b), where they were too weak to be measurable. In (c) and (d) only the points at which the one-layer diffraction patterns overlap are indicated. In (c) it is 1 in every 5, and in (d) 1 in every 29 of the one-layer reciprocal lattice points.

dimensions, but which lack the $4mm$ symmetry required of a $P422$ crystal in projection. Apparently the reason for the loss of symmetry is that the individual layers of isolated sheets are not held tightly together and tend to become displaced relative to each other by small amounts in the negative stain. No evidence has been obtained for similar effects in thin sectioned material, where presumably the native arrangement is better maintained.

Optical diffraction patterns, such as those shown in Figure 5, provide a sensitive means of demonstrating small displacements between layers. The diffraction pattern of Figure 5(a) is especially suitable for this purpose. It is from an area similar to that marked X in Figure 2. The rotation of the two layers here is the same as for the Σ_{5b} crystal, in which ideally the ribosomes in one layer form lines which are parallel and *in phase* with those of the other (see e.g. Fig. 3 and the regions where this lattice is found in Fig. 1(b)). In the diffraction pattern of a perfect Σ_{5b}-type of crystal the lines of ribosomes in each layer would therefore be expected to contribute *in phase* to the same diffraction peaks, doubling their normal amplitudes or strengthening their intensities by a factor of four. The diffraction peaks referred to index as 1.2 or -2.1 in one-layer diffraction patterns and as 0,5 or 5,0 in the diffraction pattern of a (two-layer) Σ_{5b} crystal (see Fig. 5(a)). In one-layer diffraction patterns they are the strongest peaks next to the 0,1 and the peak at the origin (see Fig. 5(b), (c) and (d)), and with a perfect Σ_{5b} crystal, therefore, we would expect them to be exceptionally strong. Figure 5(a), on the contrary, shows both the 1,2 and the -2.1 peaks to be weak in comparison with several other peaks. The contributions from both layers, instead of reinforcing, must therefore be tending to cancel, meaning that the lines of ribosomes in one layer must be fitting approximately midway between those in the other.

Numerous examples of "displaced crystals" have been found, each having essentially the same diffraction patterns as their "correct" counterparts, except, as one would expect, at those reciprocal lattice points which are shared by both layers.

(*d*) *Fourier analysis of micrographs*

In analysing the micrographs of the isolated sheets one may think of their diffraction patterns either in terms of a single crystal diffraction pattern or in terms of the superposition of two separate diffraction patterns, one arising from each layer. The second approach is obviously the preferable one, since the interest lies more in the appearance of layers than in whole sheets. The reciprocal lattice of one of the pair of diffraction patterns only coincides with that of the other at $1/\Sigma$ of its reciprocal lattice points. The indices of the points of coincidence differ according to the coincidence lattice concerned (see Table 1) and this means that, in general, any two crystals (except that for which $\Sigma = 1$) can be used to provide a complete set of diffraction data corresponding to one layer. (A single sheet where the two layers are randomly rotated with respect to each other would also be sufficient.)

Figure 5 gives some of the most commonly encountered optical diffraction patterns. Each is arranged so that the orientation of the diffraction pattern of the layer farthest from the electron source is fixed (orthogonal axes parallel to the sides of the page). The diffraction patterns from the layers nearest to the source are inverted with respect to this pattern and rotated according to the value of Σ. There are eight one-layer diffraction patterns altogether in Figure 5 and close inspection of each of them, ignoring the points of coincidence, shows that equivalent peaks have similar intensities.

A more quantitative evaluation of the separate layers was made by densitometering the micrographs corresponding to Figure 5(a) and (b), computing their Fourier transforms (see Methods), and comparing phases of each of the non-coincident peaks. After refining the phases derived from each layer on to the same origins by minimising differences between the 4-fold related peaks, mean phase errors of only 10°, 12°, 22° and 17° were obtained for the four separate cases. Equivalent peaks in each case (assuming one of the pair of diffraction patterns to be inverted with respect to

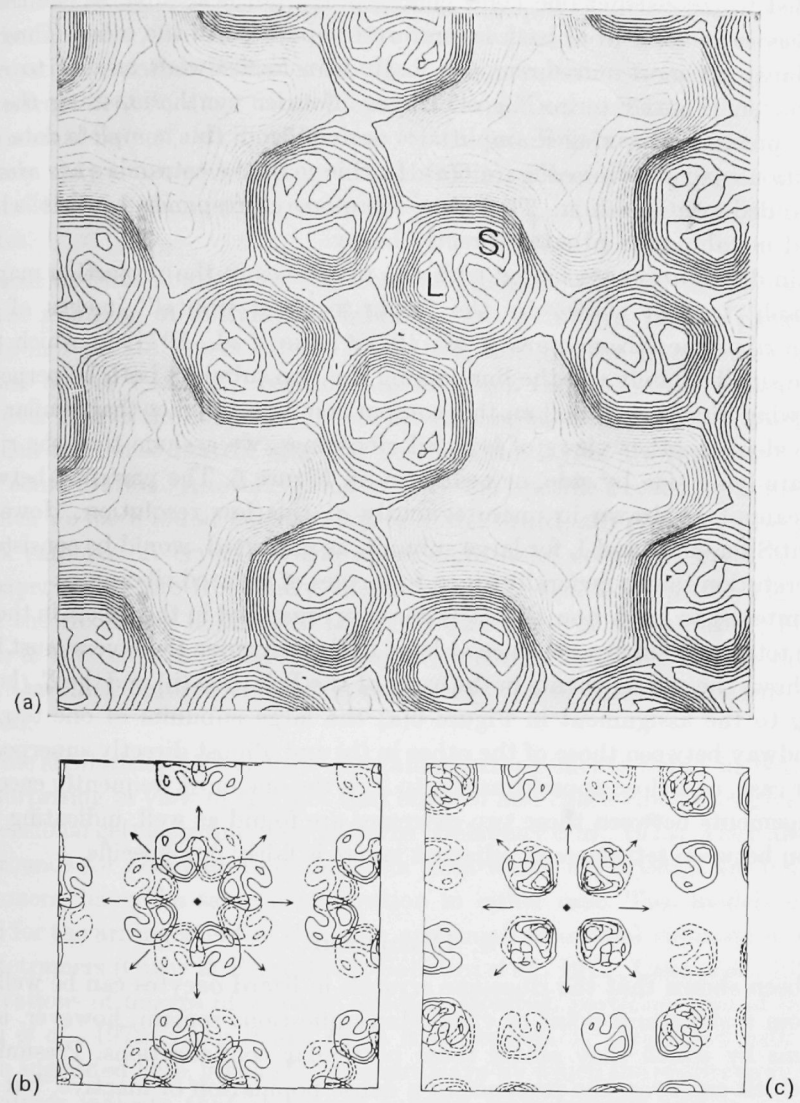

FIG. 6. Structure and packing of layers. (a) Projected structure of one layer, as seen with the juxtaposed membrane underneath. The $F(0,0)$ term was not included in the synthesis. Negative contours (i.e. stain-excluding regions) are indicated by thicker lines. The unit cell dimension, from the centre of one tetramer to that of the next, is 595 Å. The way in which each ribosome appears to be divided into its large (L) and small (S) subunits is indicated. (b) and (c) Show the relative positions of these subunits in 2 of the most frequently found $P422$ crystals, Σ_1 and Σ_{5b} lattices, respectively, at the points where the tetramers superpose. Broken lines refer to one layer and full lines to the other. The unit cell dimension of (b) is 595 Å, as for the one layer, but (c) has a much larger unit cell (a = 1330 Å) and only part of it is shown.

the other) then gave the same centrosymmetric phases. These results demonstrate unequivocally that the two layers comprising a sheet face in opposite directions and have the same structure, it being independent of the way they are organised with respect to each other.

(c) *Projected structure of one layer*

The two computed Fourier transforms just referred to together provided up to eight measurements of amplitude and phase for each crystallographically independent term needed to reconstruct one layer. Those peaks not accessible in one transform, because they originated from both layers, were separated in the other. Thus in spite of redundancy in most measurements, both transforms were needed to obtain a complete set of Fourier terms for one layer. Fourier synthesis, using the centrosymmetric phases and averaged amplitudes derived from this complete data set gave the projection map shown in Figure 6(a). In this map the tetramers are arranged in a right-handed configuration. The view therefore corresponds to that where the juxtaposed membrane is situated directly below.

The stain distribution associated with the ribosomes in the projection map corresponds closely to that shown by the "right-featured frontal" images of isolated eukaryotic ribosomes (Nonomura *et al.*, 1971; Lake *et al.*, 1974) in which the long axis of the small subunit and the line joining the two subunits both lie perpendicular to the viewing direction. Based on this comparison, and the fact that similar features are not evident in other views of isolated ribosomes, we assume that the ribosomal subunits are lying side by side, or nearly so, in Figure 6. The partition between the subunits cannot be drawn in unambiguously at this low resolution. However, the assignment S for small and L for large subunit, as indicated, would be consistent with the interpretation that is generally given to images of isolated ribosomes.

It is of interest to know how the ribosomes are organised in the sheets in the regions where the tetramers superpose, since at least in these regions the layers must interact. Figure 6 shows the arrangements in the cases of the Σ_1 lattice (b) and the Σ_{5b} lattice (c). According to the assignment in Figure 6(a) the large subunits of one tetramer lie almost midway between those of the other in (b) and almost directly superpose in (c). The latter case, or a close approximation to it, is the one most frequently encountered but arrangements between these two extremes are found as well, indicating that the interaction between tetramers in adjacent layers is fairly non-specific.

4. Discussion

It has been shown that the ribosome crystals in lizard oocytes can be well characterised from a structural point of view. Many questions remain, however, as to the mechanisms by which they attain these particular configurations. Presumably, as with the chick embryos, the presence of a dense population of inactive, but mature, 80 S ribosomes and low temperatures are requirements for crystal growth (Byers, 1971, Morimoto *et al.*, 1972*a*,*b*), but the situation is somewhat more complicated with the lizard, owing to the fact that its crystals are always associated with membranes. Another peculiarity of the lizard crystals, relevant to the mechanism of their formation, is that they never form extensive single layers as are frequently seen in the chick embryo case. Small patches of single layers are sometimes observed but apparently a second layer is required to render them stable.

Growth of the two layers, despite the need for the second layer, seems to proceed, to some extent, independently. This is suggested by thin section results which show the two layers of a sheet sometimes to be well separated by dense matrix material, and which show one of the layers of a sheet sometimes to change its orientation independently of the other (Fig. 1(b)). The findings that the two layers relate to each other in many different ways and that in isolated sheets they are easily displaced, are also indicative of weak layer to layer interaction.

The membranes may be directly responsible for bringing about the crystallisation, but it seems unlikely. One reason for believing this is that the chick embryo crystals, as we discuss below, are very similar structurally but do not require membranes for their formation. Another is that removal of the membranes from the lizard crystals by Triton treatment does not cause them to disrupt. In the chicken the crystallisation is not a normal part of cell development; in the lizard it is. It would therefore seem more likely that the membranes are involved in processes directed at maintaining normal cellular function, such as in the packaging of the crystals into compact aggregates.

The most obvious similarities between the ribosome crystals in the two animals are (1) the grouping of individual ribosomes into tetramers, (2) the packing of the tetramers in separate layers into a $P4$ lattice, and (3) the frequent occurrence in either case of the $P422$, Σ_1, relationship in which each tetramer in one layer fits directly over that in the other. But there are further likenesses. In both the lizard and the chicken the dense matrix material between the layers always "sees" the right-handed, configuration. Another point is that the specific crystallographic relationships which we have found between layers in the lizard, are probably also present in the chick embryos. A crystal in the upper right-hand corner of Plate X of Byer's (1967) paper shows the frequently encountered Σ_{5b} relationship (see Fig. 4), where many of the ribosomes in the two layers fit directly over one another; Figure 5 of O'Connor & Wyttenbach (1974) seems to show a similar example. But a more detailed study of the chick embryo crystals is really required to substantiate this suggested correlation.

The close similarities between the crystalline arrangements found in both animals are not surprising in view of the fact that chicken and lizard ribosomes give identical two-dimensional gel electrophoresis patterns (Delaunay *et al.*, 1973). They also provide strong grounds for believing that the units from which the crystals are built up, i.e. the tetramers, have the same configuration in either case. Two models have been proposed for the arrangement of the large and small ribosomal subunits in the chick embryo tetramers (Carey & Read, 1971; Sabatini *et al.*, 1972; Lake *et al.*, 1974) based on observations of images of visually selected, isolated, particles. One of the models (Sabatini *et al.*, 1972; Lake *et al.*, 1974) is in reasonable agreement with the configuration suggested here, given the different ways by which the results were obtained. Both analyses indicate that the small subunit–large subunit axis is roughly perpendicular to the central 4-fold axis. A more precise description of the organisation of the subunits within the tetramer will have to await the results of a three-dimensional analysis.

This work was supported, in part, by a European Molecular Biology Organisation short-term fellowship given to one of us (P. N. T. U.). We thank Professor A. Monroy and Dr S. Metafota, C.N.R. Laboratory of Molecular Embryology, Arco Felice, Naples, for the use of their facilities.

REFERENCES

Arndt, U. W., Barrington-Leigh, J., Mallett, J. F. W. & Twinn, K. E. (1969). *J. Sci. Instr.* **2**, 385–387.

Brandon, D. G., Ralph, B., Ranganathan, S. & Wald, M. S. (1964). *Acta Metallurgica*, **12**, 813–821.

Byers, B. (1967). *J. Mol. Biol.* **26**, 155–167.

Byers, B. (1971). *Proc. Nat. Acad. Sci., U.S.A.* **68**, 440–444.

Carey, N. H. & Read, G. S. (1971). *Biochem. J.* **121**, 511–519.

Delaunay, J., Creusot, F. & Schapira, G. (1973). *Eur. J. Biochem.* **39**, 305–312.

DeRosier, D. J. & Moore, P. B. (1970). *J. Mol. Biol.* **52**, 355–369.

Erickson, H. P. & Klug, A. (1971). *Phil. Trans. Roy. Soc. ser B*, **261**, 105–118.

Holloway, P. W. (1973). *Anal. Biochem.* **53**, 304–308.

Lake, J. A., Sabatini, D. D. & Nonomura, Y. (1974). In *Ribosomes* (Nomura, M., Tissières, A. & Lengyel, P., eds), pp. 543–557, Cold Spring Harbor Laboratory Press, New York.

Morimoto, T., Blobel, G. & Sabatini, D. D. (1972*a*). *J. Cell Biol.* **52**, 338–354.

Morimoto, T., Blobel, G. & Sabatini, D. D. (1972*b*). *J. Cell Biol.* **52**, 355–366.

Nonomura, Y., Blobel, G. & Sabatini, D. D. (1971). *J. Mol. Biol.* **60**, 303–323.

O'Connor, T. M. & Wyttenbach, C. R. (1974). *J. Cell Biol.* **60**, 448–459.

Sabatini, D., Nonomura, Y., Morimoto, T., Blobel, G. & Ulrich, B. L. (1972). *FEBS Symp.* **23**, 147–173.

Taddei, C. (1972). *Exp. Cell Res.* **70**, 285–292.

Taddei, C. & Filosa, S. (1976). *Exp. Cell Res.* **102**, 416–419.

Taddei, C., Gambino, R., Metafota, S. & Monroy, A. (1973). *Exp. Cell Res.* **78**, 159–167.